~~RESTRICTED~~ UNCLASSIFIED

RM E51H06

NACA RM E51H06

C.1

NACA

RESEARCH MEMORANDUM

34 units

ANALYTICAL INVESTIGATION OF FLOW THROUGH HIGH-SPEED MIXED-FLOW TURBINE

By Warner L. Stewart

Lewis Flight Propulsion Laboratory
Cleveland, Ohio

NATIONAL ADVISORY COMMITTEE
FOR AERONAUTICS

WASHINGTON
October 3, 1951

~~RESTRICTED~~ UNCLASSIFIED

NACA RM E51H06

NATIONAL ADVISORY COMMITTEE FOR AERONAUTICS

RESEARCH MEMORANDUM

ANALYTICAL INVESTIGATION OF FLOW THROUGH HIGH-SPEED MIXED-FLOW TURBINE

By Warner L. Stewart

SUMMARY

An analysis was made of the flow through a mixed-flow turbine designed to drive a high-speed, high-weight-flow compressor, of the type that could be used in supersonic aircraft. The analysis, which is based on axially symmetric flow, was developed from a method previously used to predict trends of flow in mixed-flow compressor impellers to include an analysis of the region downstream of the rotor. Results of the analysis indicate that the weight flow calculated by this three-dimensional method is lower than that weight flow used in the two-dimensional design of the turbine. The results also indicate that redesign of the inner wall of the rotor can provide sufficient flow area to allow design weight flow to pass and to alleviate the adverse velocity and pressure gradients indicated in the analysis at the expense of increased rotor blade stresses.

INTRODUCTION

The development of high-speed, high-weight-flow transonic and supersonic compressors particularly for high-speed aircraft is dependent on the proper design of turbines to drive these compressors. In order to determine the problems involved, a turbine was designed at the NACA Lewis laboratory to drive a supersonic compressor that could be installed in a supersonic aircraft.

The high rotational speed and high-weight-flow characteristic of these compressors caused high turbine rotor blade stresses, which were minimized by making the rotor blades highly tapered and the annulus area at each station through the rotor as small as practical from aerodynamic considerations. The resulting turbine configuration is of the mixed-flow type having a high degree of insweep of the inner wall.

Since no general method of designing mixed-flow turbines is available, the preliminary rotor blade design was based on two-dimensional flow and the effect of the hub-shroud profile and blade taper was neglected. The large hub-shroud insweep and blade taper of this turbine type, however, indicated the need for additional information on the effects they would have on the flow. A method is presented in reference 1 for computing the flow through a mixed-flow compressor rotor. Based on axially symmetric flow and utilizing a numerical solution and an iteration process, the method is also applicable to the calculation of the flow through mixed-flow turbine rotors. Good experimental correlation of the analytical results was obtained for the compressor even though isentropic flow and axial symmetry were assumed (reference 1). In order to determine the flow through the turbine being investigated, however, it was necessary to extend the method of reference 1 to include the flow downstream of the rotor since the large blade taper and hub-shroud curvature caused downstream conditions which affected the flow inside the rotor.

The investigation applies this extended method to the mixed-flow turbine, examines the flow conditions indicated by the solution, and evaluates the method in regard to information not obtainable by two-dimensional methods.

TURBINE CONFIGURATION

The turbine design was on a two-dimensional basis and utilized free-vortex entry with zero exit whirl. For a given turbine diameter and weight flow per unit frontal area, there is a hub-tip ratio at which the minimum entering relative Mach number at the hub occurs. At hub-tip ratios above this point, the relative Mach number is higher because of high axial velocities while at hub-tip ratios below this point the relative Mach number is higher because of high whirl velocities. As the weight flow per unit frontal area of the turbine is decreased this minimum Mach number becomes lower. In this design the weight flow per unit frontal area of the turbine was decreased until minimum relative Mach number entering the rotor at the hub corresponding to this weight flow per unit frontal area reached a practical limit from aerodynamic considerations. The hub-tip ratio corresponding to this minimum relative Mach number was then used in the design.

The hub and tip velocity diagrams are shown in figure 1. At the two sections shown, a mean camber line was drawn to give a slight angle of incidence and a small amount of overturning. An airfoil was then wrapped about each of these mean camber lines. The cross-sectional area of the blade profile at the tip was made 30 percent of that at the root to provide large blade taper and thereby minimize stresses. This

design necessitated high solidities at the root and low solidities at the tip. A sketch of the rotor blades and the two sections used in the design are shown in figure 1. The flow passages at the two sections were made to converge toward the exit. The two sections were stacked and the blade was formed by fairing in straight lines between the two sections. Since the hub radius at the inner wall was different at the exit from that at the entrance, these two radii were joined by a smooth curve. The rotor blade shape was therefore determined from inlet and exit conditions only, and the effects of the high degree of taper and insweep of the inner wall on the flow characteristics within the rotor were neglected.

ANALYSIS

The method of analysis used in this report is similar to that presented in reference 1. The differential equations used to compute the velocity distribution within the rotor are the same. All symbols used are defined in appendix A. In order to complete the analysis of the flow downstream of the rotor, a differential equation yielding the velocity distribution downstream is derived in appendix B.

Assumptions. - The following assumptions were made in the method of analysis used in this report:

(1) The flow is nonviscous and compressible and the flow process isentropic.

(2) Axially symmetric conditions are assumed to exist throughout the turbine flow annulus.

(3) The flow is assumed to follow the mean camber surface of the rotor blades. This assumption is valid near the hub because of the high solidity but is only approximate near the tip where the solidity is low.

(4) The surfaces of the rotor blades are so nearly radial that the radial component of the blade force can be neglected.

(5) The rotor blade is assumed to extend to the outer wall.

(6) A wake is assumed to exist a short distance downstream of the rotor blades so there will be no sharp change in flow area at the exit. This assumption approaches the physical case and insures a smooth streamline configuration. Because of the rapid change in flow area at the entrance to the rotor, the results of the analysis are only approximate in this region.

Final equations. - The differential equation (8) of reference 1 must be solved to determine the variation in velocity along an orthogonal inside the rotor. The nozzle-exit flow configuration is free-vortex so $\frac{\partial\lambda}{dn} = 0$ and equation (8) applies. This equation is written as

$$\frac{dq}{dn} = aq - b \tag{1}$$

where

$$a = \frac{\cos^2\beta}{r_c} - \frac{\sin^2\beta}{r}\cos\alpha - \frac{\sin^2\beta}{r}\tan\alpha\sin\alpha$$

$$b = 2\omega\sin\beta\cos\alpha + \sin\beta\tan\alpha\left(2\omega\sin\alpha + \frac{du}{dm}\right)$$

Appendix B gives the derivation of the differential equation which, when solved, yields the variation in velocity along an orthogonal downstream of the rotor. This equation (B6) is

$$\frac{d(v^2)}{dn} = A(v)^2 - B \tag{2}$$

where

$$A = \frac{2}{r_c}$$

$$B = 2\left[\left(\frac{K}{r^2} - \omega\right)\frac{dK}{dn}\right]$$

Both differential equations (1) and (2) are of the form

$$\frac{dy}{dx} + Ry = S$$

so the solutions of these equations are

$$q = e^{\int_{n_o}^{n} a\,dn}\left(q_o - \int_{n_o}^{n} b\,e^{-\int_{n_o}^{n} a\,dn}\,dn\right) \tag{3}$$

and

$$v^2 = e^{\int_{n_o}^{n} A\,dn}\left((v_o)^2 - \int_{n_o}^{n} B\,e^{-\int_{n_o}^{n} A\,dn}\,dn\right) \tag{4}$$

Since $v = q \cos \beta$ equation (10) of reference 1 can be written as

$$w = 2\pi \int_{n_o}^{n} rf\rho gv\,dn \tag{5}$$

and can be used to calculate the weight flow crossing orthogonals inside and downstream of the rotor. The density can be computed from equation (11) in reference 1, which is rewritten here

$$\rho = \rho_{T,i}\left\{1 + \frac{\gamma-1}{2}\left[\left(\frac{\omega r}{c_i}\right)^2 - \left(\frac{q}{c_i}\right)^2\right] - \frac{\omega\lambda}{gH_i}\right\}^{\frac{1}{\gamma-1}} \tag{6}$$

Application of equations to turbine. - The application of the preceding equations to the mixed-flow turbine was quite similar to that used in the analysis of mixed-flow compressors. A plot similar to figure 2 was first made of the projection of the rotor and flow passage in a meridional plane (including the axis of rotation). Superimposed on this plot were lines of constant r, z, φ, and f. A number of streamlines and orthogonals was then drawn in. At the inlet the position of these streamlines was located so that equal weight flow increments passed between each pair. Because of free-vortex entrance conditions, the axial velocity was constant and the whirl component varied inversely as the radius. The coefficients a, A, b, and B were then determined at the intersections of the streamlines and orthogonals by selecting values of r, z, φ, and f, measuring the slope of the streamlines to obtain α, and calculating the radius of curvature r_c. Since K is constant along a streamline downstream of the rotor, it was calculated from conditions at the exit of the rotor.

The radius of curvature was calculated by means of a radometer, which was developed especially for this type of analysis. The accuracy

of this method was comparable with that obtained in the method used in reference 1 and shortened the calculation time considerably. The instrument and its principles are described in appendix C. The angle β was calculated from φ and α by the equation

$$\tan \beta = \cos \alpha \tan \varphi$$

In the first trial $\frac{du}{dm}$ was neglected. For subsequent trials, values of this quantity were taken from the preceding trial.

Three types of orthogonal were encountered in the analysis. The following procedures were used to find the velocity distribution along each type:

(a) Orthogonal completely inside rotor. The velocities along an orthogonal completely inside the rotor were found by assuming a velocity at the hub and solving equation (3) along the orthogonal by the trapezoidal method. The resulting velocities were used to find ρ at each point by equation (6) and hence the weight flow by equation (5). Various hub velocities were assumed and total weight flow was plotted against assumed hub velocity. If the design weight flow could pass, the velocity distribution corresponding to this weight flow could be used. In this analysis, the choking weight flow occurred along the orthogonal originating at A in figure 2 and was less than the design value. Hence the weight flow across all the other orthogonals had to be the same and the corresponding velocity distribution used.

(b) Orthogonal part inside rotor and part downstream of rotor. The procedure for this type of orthogonal was slightly more complicated than for the type completely within the rotor. A velocity was first assumed at the hub. By use of equation (3), the velocity distribution along the orthogonal was computed up to the trailing edge and K computed at this point. The value of K had previously been calculated at the intersection of the preceding orthogonal and the trailing edge. In the case of the first orthogonal including flow inside and downstream of the rotor, the previous orthogonal was the one originating at the point A in figure 2. A linear variation in K was then assumed between the two points yielding values of K for the streamlines crossing the orthogonal downstream of the rotor. As more orthogonals were used, this assumption became more accurate. By use of the velocity obtained at the trailing edge as the lower limit of integration, equation (4) was solved for the velocity distribution along that part of the orthogonal downstream of the rotor. The densities were then computed by equation (6) and used to calculate the total weight flow by equation (5) for the assumed hub velocity. The process was then repeated for various values of hub velocities until the total weight flow checked with design or choking value.

(c) Orthogonal downstream of rotor. The velocity distribution along an orthogonal downstream of the rotor was found by equation (4), the same procedure being used as for the orthogonal inside the rotor. The parameter K was completely determined in the application of part (b).

The positions of the streamlines upstream of the rotor were determined so that equal weight-flow increments existed between each pair. A new streamline configuration was then determined so that this condition existed through and downstream of the rotor. The positions of these new streamlines were obtained by dividing the weight flow crossing an orthogonal into the required number of weight-flow increments. Once these positions were found for each orthogonal, the new set of streamlines was drawn and the entire process repeated for this new streamline configuration. The iteration procedure continued until the weight flows between all pairs of streamlines were identical and the total weight flows across all orthogonals were the same. Once the final positions of the streamlines were known, the pressure distribution throughout the flow field was calculated by the isentropic relation $\frac{p}{\rho^{\gamma}}$ = constant. The velocity and pressure distribution then could be examined for possible adverse gradients and the effect of the hub-shroud profile on the flow characteristics determined.

RESULTS AND DISCUSSION

Choking within rotor. - The high-speed turbine was designed to pass an equivalent weight flow of 15.3 pounds per second. However, the analysis indicated that the rotor choked at 14.7 pounds or 96 percent of design weight flow. This weight flow was obtained under isentropic flow conditions with no boundary layer. In the actual turbine, the total pressure through the turbine drops because of losses and a certain amount of boundary-layer build-up exists which will further lower the weight flow. This result indicates that the design of this type of turbine by two-dimensional methods will yield a turbine incapable of passing the design weight flow. Because of the shape of the inner wall, the area perpendicular to the flow along the choking orthogonal is insufficient. For a fixed outer diameter the hub profile would have to be redesigned to provide more flow area so that the desired weight flow could be passed. In the present computation, the rotor inlet conditions had to be changed so that the weight flow was equal to the choking value. Also, the choking condition was indicated in the first trial solution and further trials did not affect the choking position or value. Hence, only one trial would be needed to determine whether or not the design weight flow could be passed for a given turbine configuration.

Streamline configuration. - The streamline configuration obtained in the analysis of the high-speed turbine is shown in figure 3. The streamlines were chosen so that 1/10 of the weight flow passed between each pair of streamlines. Downstream of the rotor near the hub, the distance between the streamlines indicates that the small radius of curvature at the inner shroud and divergence of the streamlines introduces adverse velocity and pressure gradients in this region. This occurrence will be shown more clearly in the plots of the velocity and pressure ratios.

Local Mach number within rotor. - The local Mach number distribution within the rotor determined by the analysis is shown in figure 4. The orthogonal where choking occurred is shown on the figure. The local Mach number is not unity across the orthogonal but varies from subsonic velocities near the hub to supersonic velocities near the tip.

Static-pressure distribution. The static-pressure distribution calculated in the analysis is shown in figure 5. Lines of constant P_r are plotted where P_r is defined as the ratio of static pressure at any point to total pressure at the inlet. Within the rotor, the gradients are exactly the opposite of the velocity gradients of figure 4. Along the outer wall, a rapid drop in static pressure yields a favorable pressure gradient. Along the inner wall, however, the static pressure reaches a minimum in the choking region. A positive pressure gradient then occurs along the inner wall near the exit of the blade. This adverse pressure gradient continues to the sharp bend just downstream of the rotor. Because a positive pressure gradient induces boundary-layer build-up and separation, the analysis indicates that separation would probably take place and the boundary of the flow would follow a path approximated by the dashed line indicated in figure 5. An adverse pressure gradient also exists along the outer wall downstream of the rotor, which indicates possible boundary-layer growth in this region.

Design indications. - The results of the analysis indicate possible modifications of the mixed-flow turbine investigated.

(1) Within the rotor, the inner radius could be decreased to provide the necessary flow area to allow design weight flow to pass, which would increase rotor blade stresses.

(2) The sharp bend just downstream of the rotor could be smoothed out somewhat to reduce the positive pressure gradient along the inner wall.

(3) If the hub-tip ratio at the outlet were maintained and the hub-tip ratio within the rotor reduced to provide more flow area in the region of choking, the sharp bend would automatically be reduced

considerably. Also, the positive pressure gradients occurring downstream of the rotor at the tip and within the rotor at the hub would be diminished because the inner and outer walls diverge less. The resulting rotor blade stress would be increased by the increased annulus area.

Evaluation of results. - Because of the assumption of axial symmetry, the results of the analysis apply to the middle of the flow passages within the rotor. Along the pressure surface, the velocities will be lower than indicated by the analysis while the velocities on the suction surface will be higher. Downstream of the rotor, the results should be representative of the whole annulus.

The results of the analysis indicate that a design method based solely on inlet and outlet conditions is unsatisfactory for turbines of this type. An accurate study of the area perpendicular to the flow within the rotor should be made to insure sufficient flow area for the design weight flow. In a design an orthogonal could be sketched similar to that in figure 4 and by examination of the flow area corresponding to this orthogonal, a reasonably accurate prediction could be made as to whether or not design weight flow would be passed.

Differential equations (1) and (2), show why small radii of curvature, such as that at the exit of the turbine along the inner wall, should be avoided. The radius of curvature r_c appears in the denominators necessitating large velocity and pressure gradients along the orthogonals when r_c is small. If the configuration of the inner wall had been designed so that r_c was large, the high-pressure peak would have been modified considerably.

SUMMARY OF RESULTS

The results of the analysis of the mixed-flow turbine can be summarized as follows:

1. The analysis of the mixed-flow turbine by the three-dimensional method used in this report yields lower weight flows than those used in the design of the turbine by two-dimensional methods.

2. The choking condition or the inability of the turbine to pass design weight flow, was indicated in the first trial solution. Refinements made in further trials did not affect the choking weight flow to any extent.

3. Adverse velocity and pressure gradients occurred along the inner wall of the rotor toward the trailing edge and along the outer wall just downstream of the rotor.

4. The relatively sharp bend in the inner wall just downstream of the rotor investigated resulted in large velocity and pressure gradients in this region and can be attributed to the small radius of curvature that the flow must have to follow the wall.

5. Redesign of the inner wall would provide sufficient flow area to pass design weight flow and alleviate the adverse velocity and pressure gradients encountered in the original design at the expense of increased rotor blade stress.

CONCLUDING REMARKS

The analysis of the high-speed turbine presented in this report yielded information concerning the effects of the inner and outer wall profiles and blade shape on the choking weight flow, velocity and pressure gradients, and location of probable boundary-layer build-up and flow separation. On the basis of knowledge of these conditions, modification of the design can be made to alleviate undesirable characteristics encountered in mixed-flow turbines of this type.

Lewis Flight Propulsion Laboratory
National Advisory Committee for Aeronautics
Cleveland, Ohio

APPENDIX A

SYMBOLS

The following symbols are used in this report:

A	parameter, $\frac{2}{r_c}$
a	parameter, $\frac{\cos^2\beta}{r_c} - \frac{\sin^2\beta}{r}\cos\alpha - \frac{\sin^2\beta}{r}\tan\alpha\sin\alpha$
B	parameter, $2\left[\left(\frac{K}{r^2} - \omega\right)\frac{dK}{dn}\right]$
b	parameter, $2\omega\sin\beta\cos\alpha + \sin\beta\tan\alpha\left(2\omega\sin\alpha + \frac{du}{dm}\right)$
c	speed of sound at stagnation conditions, ft/sec
f	blade-thickness factor, $1 - \frac{Nt}{2\pi r}$
g	acceleration due to gravity, ft/sec^2
H	absolute total enthalpy, ft-lb/lb
h	static enthalpy, ft-lb/lb
K	parameter, $(r\omega + u)r$
M	local Mach number
m	distance along streamline in meridional direction, ft
N	number of blades
n	distance along orthogonal in meridional plane, ft
P_r	ratio of static pressure at any point to total pressure at inlet
p	static pressure, lb/sq ft
q	total velocity relative to rotor, ft/sec
r	radius measured from axis of rotation, ft
r_c	radius of curvature of streamline projection in meridional plane, ft

t blade thickness in circumferential direction, ft

u tangential velocity relative to rotor, ft/sec

V absolute velocity, ft/sec

v through flow component of velocity, ft/sec

w weight flow, lb/sec

z distance along axis of rotation, ft

α angle between tangent to streamline in meridional plane and axis of rotation, deg

β angle between relative velocity and component of relative velocity along streamline in meridional plane, deg

γ ratio of specific heats

λ prerotation term, $r_i (\omega r_i + u_i)$

ρ static density, slugs/cu ft

ρ_T total density, slugs/cu ft

φ blade angle in axial-tangential direction, deg

ω angular velocity of turbine rotor, radians/sec

Subscripts:

i turbine inlet

o lower limit of integration

APPENDIX B

DERIVATION OF VELOCITY EQUATION

DOWNSTREAM OF ROTOR

After the flow leaves the rotor, the moment of momentum is constant along any particular streamline. Hence

$$K = r(u + r\omega)$$

Squaring and solving for $(u + r\omega)^2$

$$(u + r\omega)^2 = \frac{K^2}{r^2} \tag{B1}$$

Although K is constant along a single streamline, in general it varies from one streamline to another. If the derivative of equation (B1) is taken with respect to n the following equation is obtained:

$$\frac{d(u + r\omega)^2}{dn} = -\frac{2K^2}{r^3}\frac{dr}{dn} + \frac{2K}{r^2}\frac{dK}{dn} \tag{B2}$$

Equation (B3) of reference 1 can be written for the region downstream of the rotor with the blade force equal to zero.

$$\frac{1}{\rho}\frac{dp}{dn} = \frac{(u + r\omega)^2}{r}\cos\alpha - \frac{v^2}{r_c}$$

or using equation (B1)

$$\frac{1}{\rho}\frac{dp}{dn} = \frac{K^2}{r^3}\cos\alpha - \frac{v^2}{r_c} \tag{B3}$$

The total enthalpy along a streamline can be related to the inlet total enthalpy by the equation

$$H = H_i - \frac{\omega}{g}(\lambda - K)$$

Differentiating with respect to n

$$\frac{dH}{dn} = \frac{dH_i}{dn} - \frac{\omega}{g}\left(\frac{d\lambda}{dn} - \frac{dK}{dn}\right) \tag{B4}$$

Also, in general, at any point on the streamline the total enthalpy can be written

$$H = h + \frac{1}{2g}\left((u + r\omega)^2 + (v)^2\right)$$

Differentiating with respect to n and noting that

$$\frac{dh}{dn} = \frac{1}{\rho g}\frac{dp}{dn}$$

$$\frac{dH}{dn} = \frac{1}{\rho g}\frac{dp}{dn} + \frac{1}{2g}\left(\frac{d(u + r\omega)^2}{dn} + \frac{d(v)^2}{dn}\right) \tag{B5}$$

Substituting equations (B2), (B3), and (B4) in equation (B5) and noting that for the turbine investigated $\frac{d\lambda}{dn} = 0$ and $\frac{dH_i}{dn} = 0$,

$$\frac{d(v^2)}{dn} - \frac{2}{r_c}(v^2) = 2\omega\frac{dK}{dn} - \frac{2K}{r^2}\frac{dK}{dn}$$

or

$$\frac{d(v^2)}{dn} = A(v^2) - B \tag{B6}$$

where

$$A = \frac{2}{r_c}$$

$$B = 2\left[\left(\frac{K}{r^2} - \omega\right)\frac{dK}{dn}\right]$$

The differential equation (B6) when solved along an orthogonal downstream of the rotor yields the variation in velocity along the orthogonal.

APPENDIX C

DESCRIPTION OF PRINCIPLE AND OPERATION OF RADOMETER

The radometer is an instrument developed to determine the radii of curvature of continuous curves such as the streamlines in this analysis. Figure 6 illustrates the principle on which this instrument is based. A smooth curve is represented by AB and the radius of curvature of this curve is to be determined at the point C. The assumption is made that the points D and E equidistant on either side of C are selected close enough together to exclude the possibility of inflection points or appreciable variation of curvature occurring between them. In this manner, a circle with radius approximating the radius of curvature of the curve at C may be passed through the points D, C, and E.

Using the nomenclature in the figure, the following equation can be written

$$\sin \frac{\delta}{2} = \frac{d}{2r_c}$$

For a given d the preceding equation can be solved for r_c in terms of δ. Thus, if δ is measured, r_c can be easily calculated.

The radometer facilitates a reasonably accurate and fast determination of δ for a given d. A photograph of this instrument is shown in figure 7. When the radometer is in use, the point O is placed over the point on the curve at which the radius of curvature is to be determined. The stationary base is oriented so that E lies on the curve. The distance OE represents d. The arm is rotated until the point D also lies on the curve. The angle δ is then read and by referring to a graph of r_c against δ for various values of d the radius of curvature can be obtained.

As mentioned in the text of the report, this method proved to be as accurate as the slope method. The accuracy of both methods decreases as the radius of curvature becomes quite small or quite large.

REFERENCE

1. Hamrick, Joseph T., Ginsburg, Ambrose, and Osborn, Walter, M.: Method of Analysis for Compressible Flow Through Mixed-Flow Centrifugal Impellers of Arbitrary Design. NACA TN 2165, 1950.

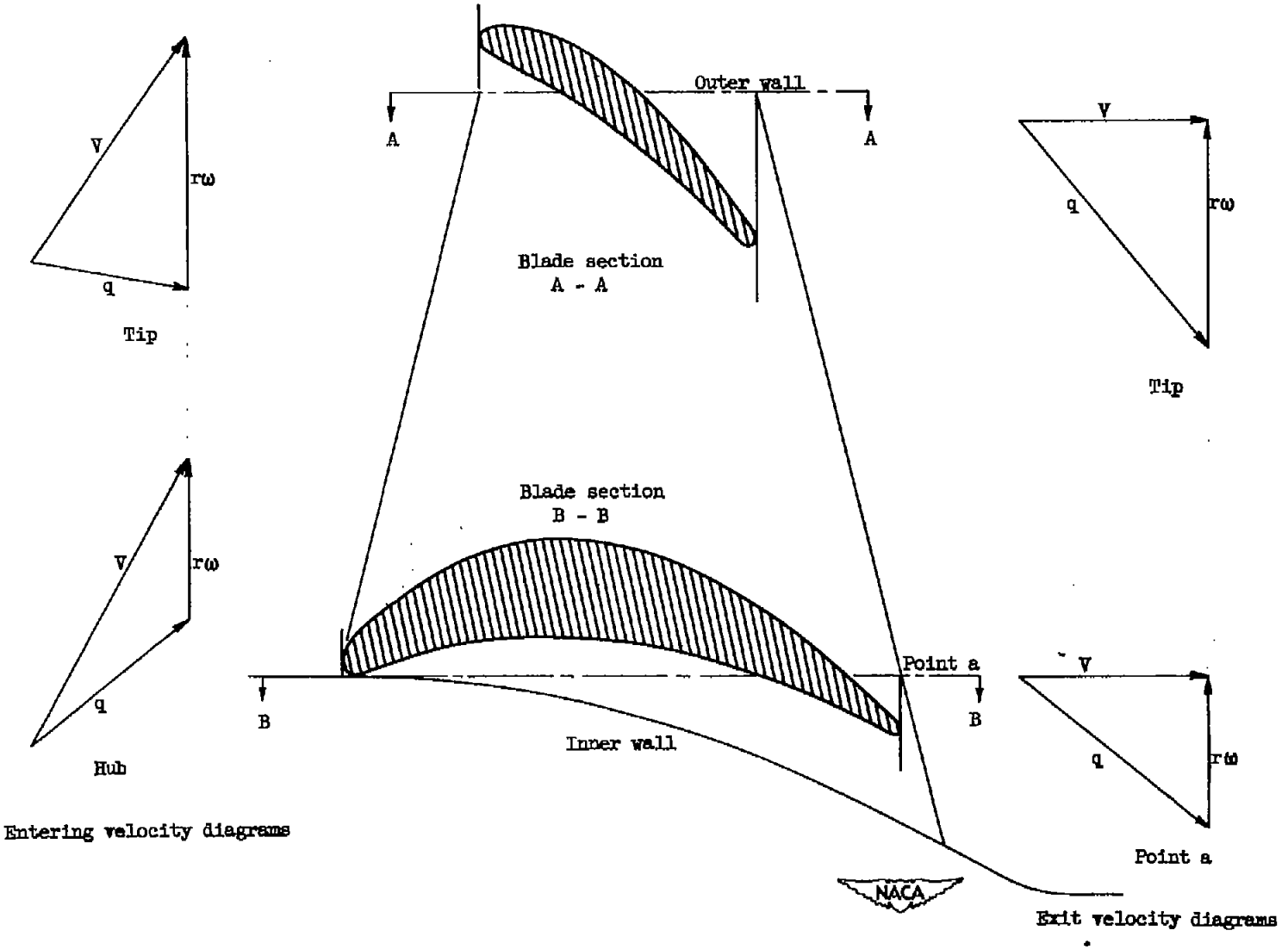

Figure 1. - Rotor blade sections and velocity diagrams used in turbine design.

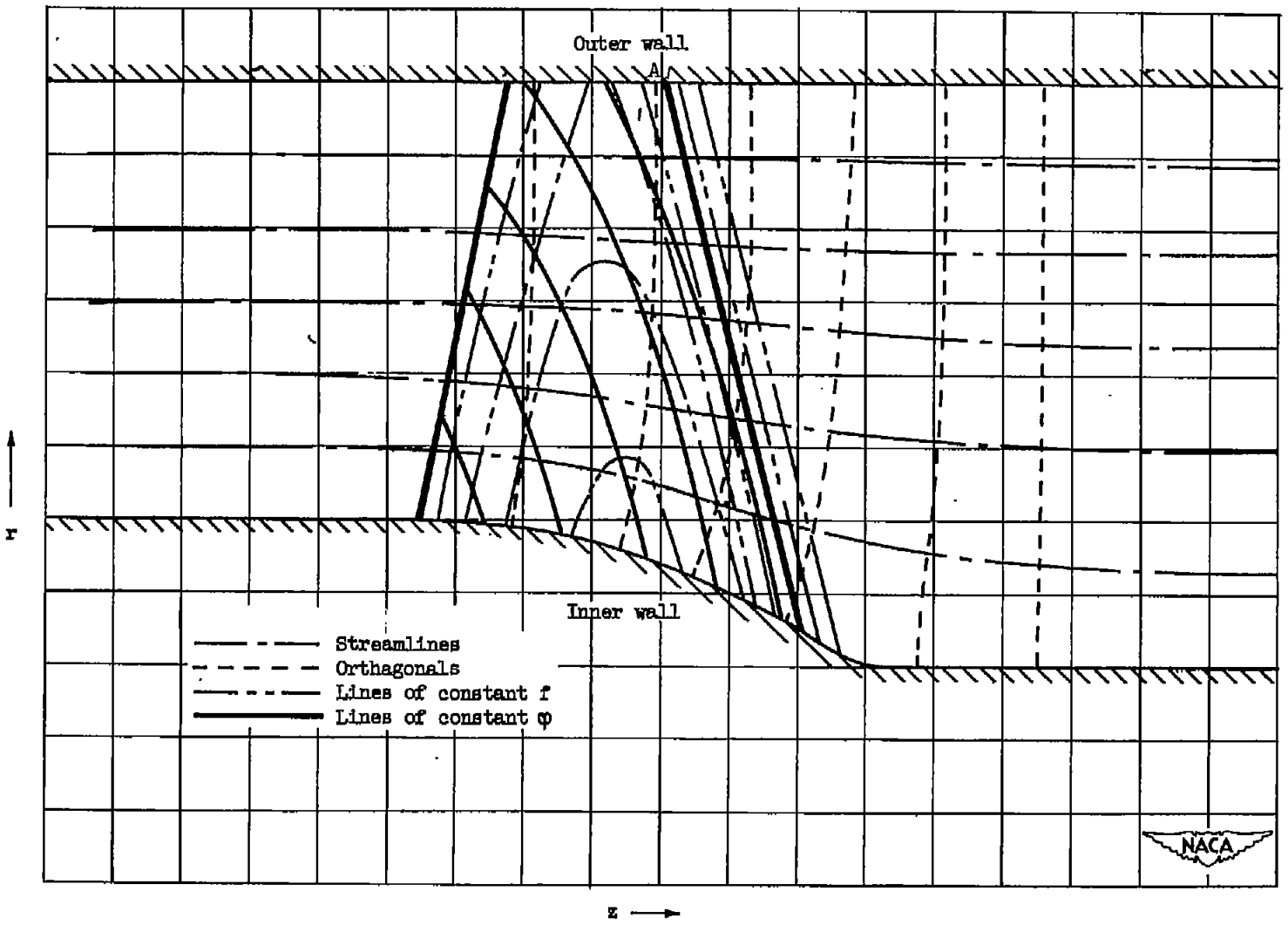

Figure 2. - Layout of method of graphically determining r, z, φ, and f at any point. A typical streamline estimate is shown.

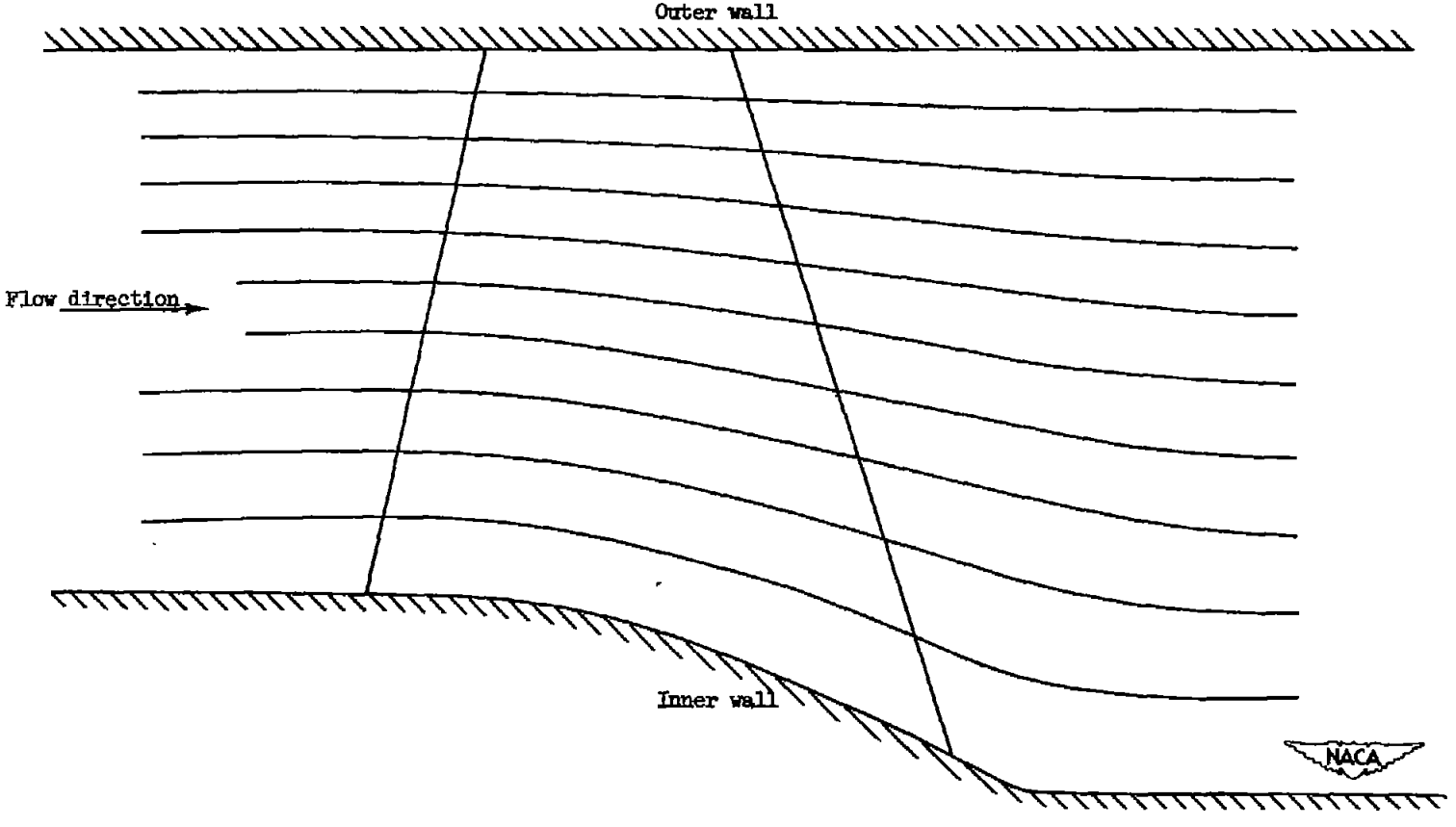

Figure 3. - Streamline configuration resulting from turbine analysis.

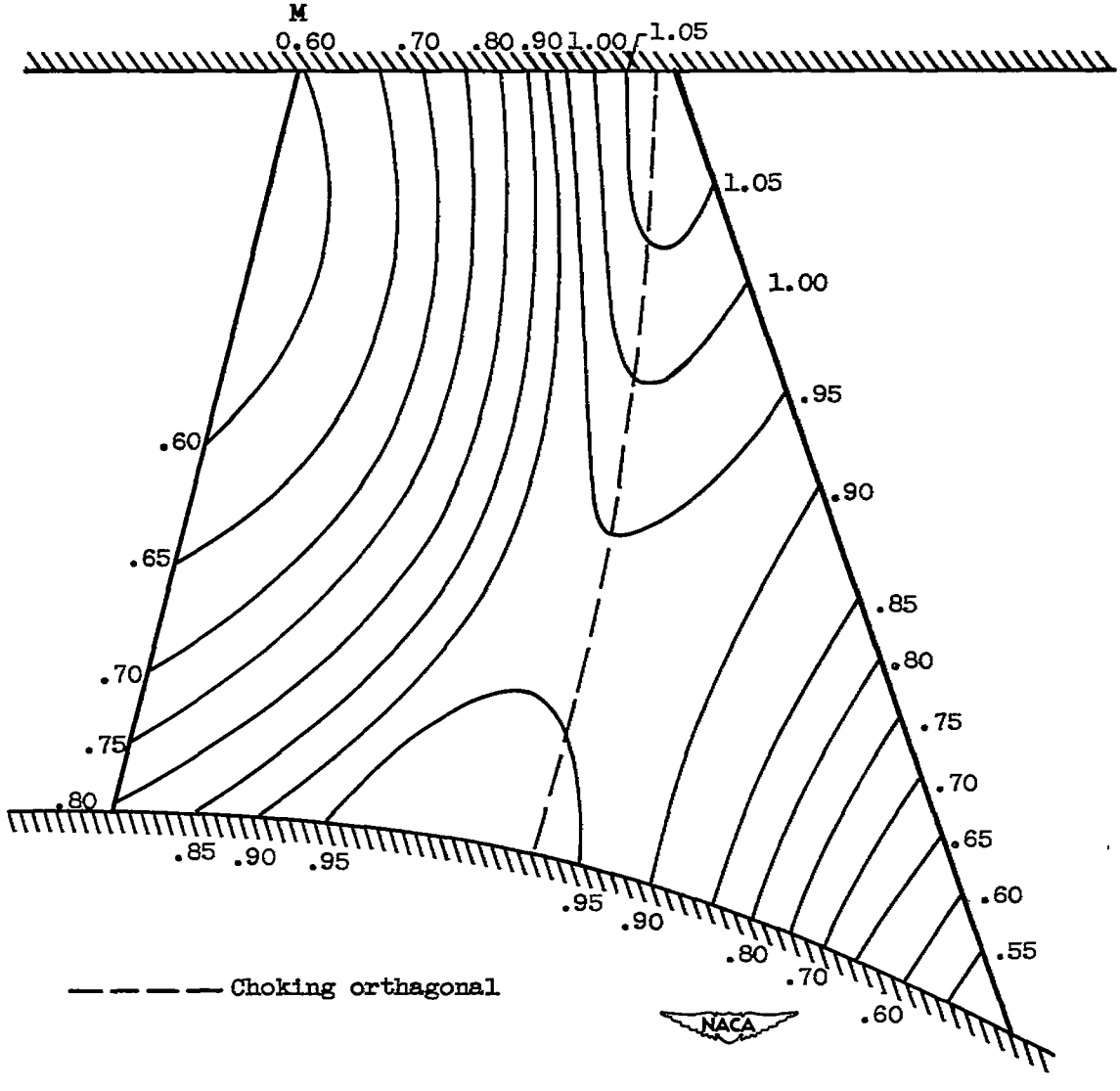

Figure 4. - Variation of local Mach number within turbine rotor.

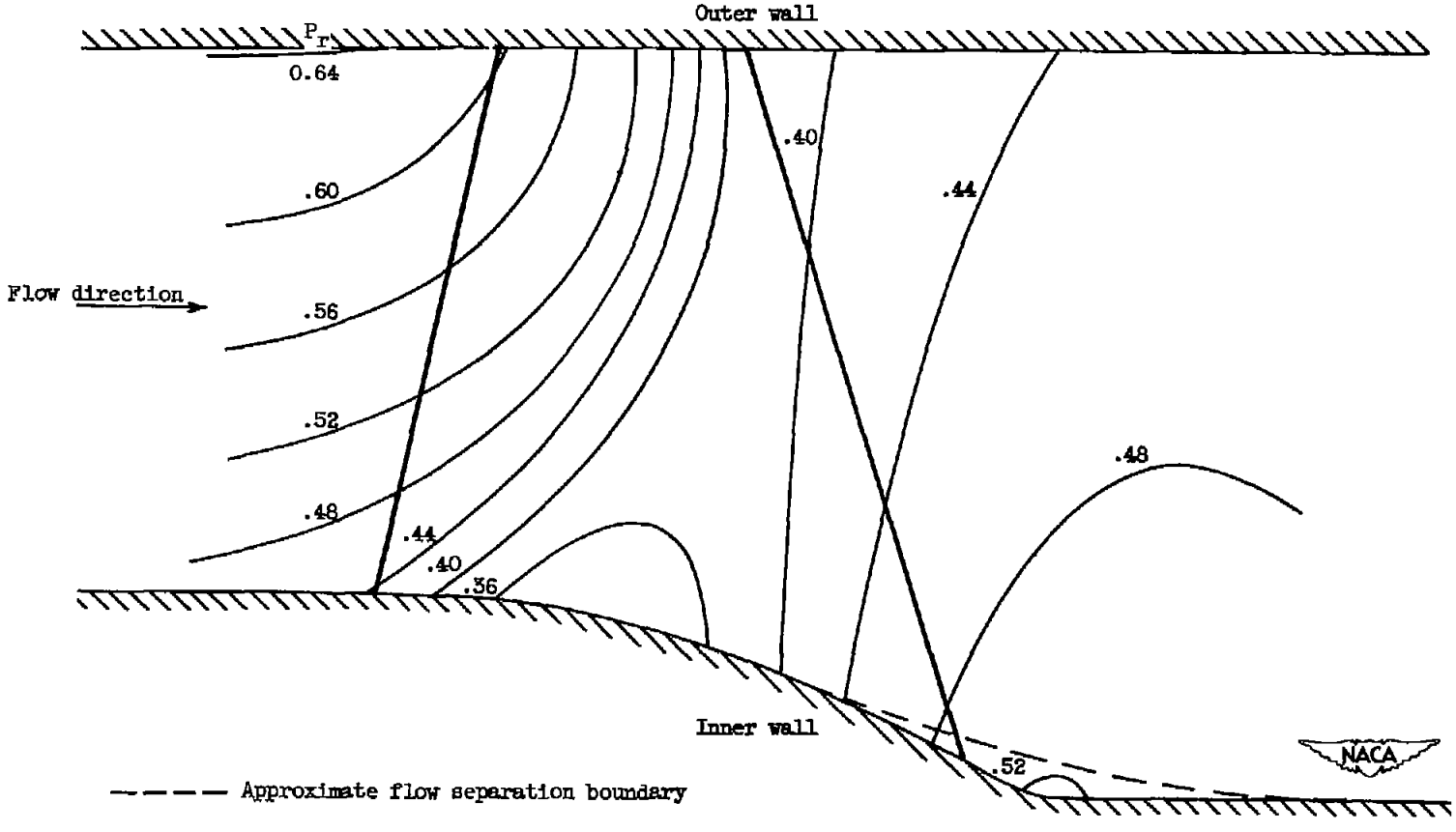

Figure 5. - Static-pressure distribution obtained in turbine analysis.

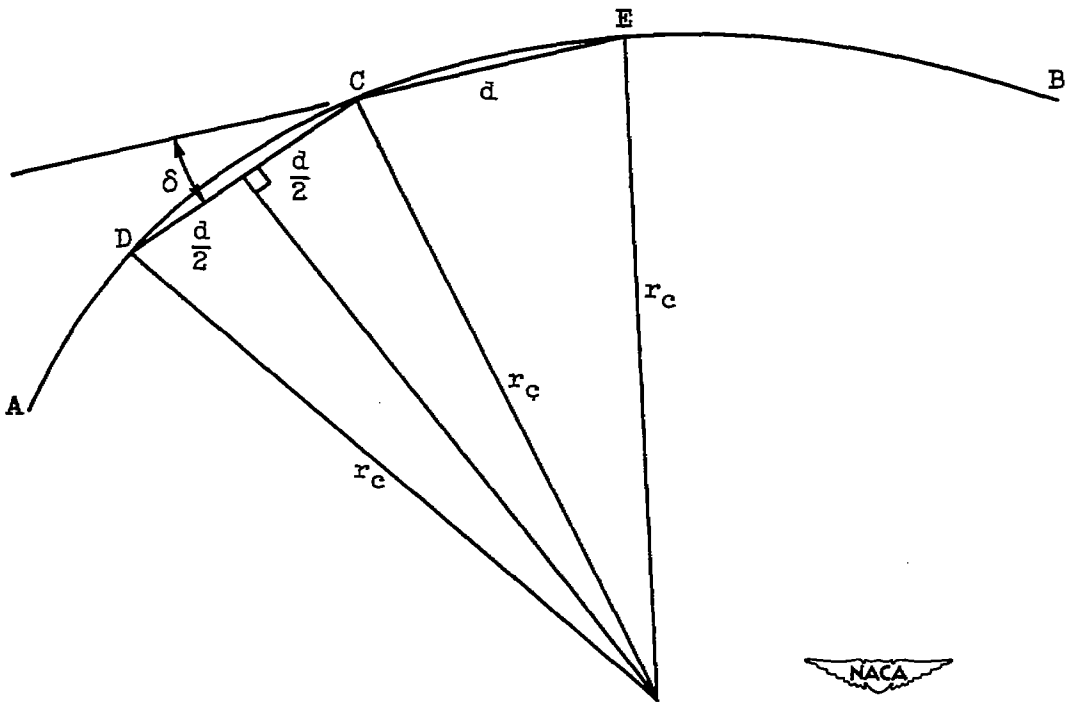

Figure 6. - Symbols used and geometric interpretation of radometer operation.

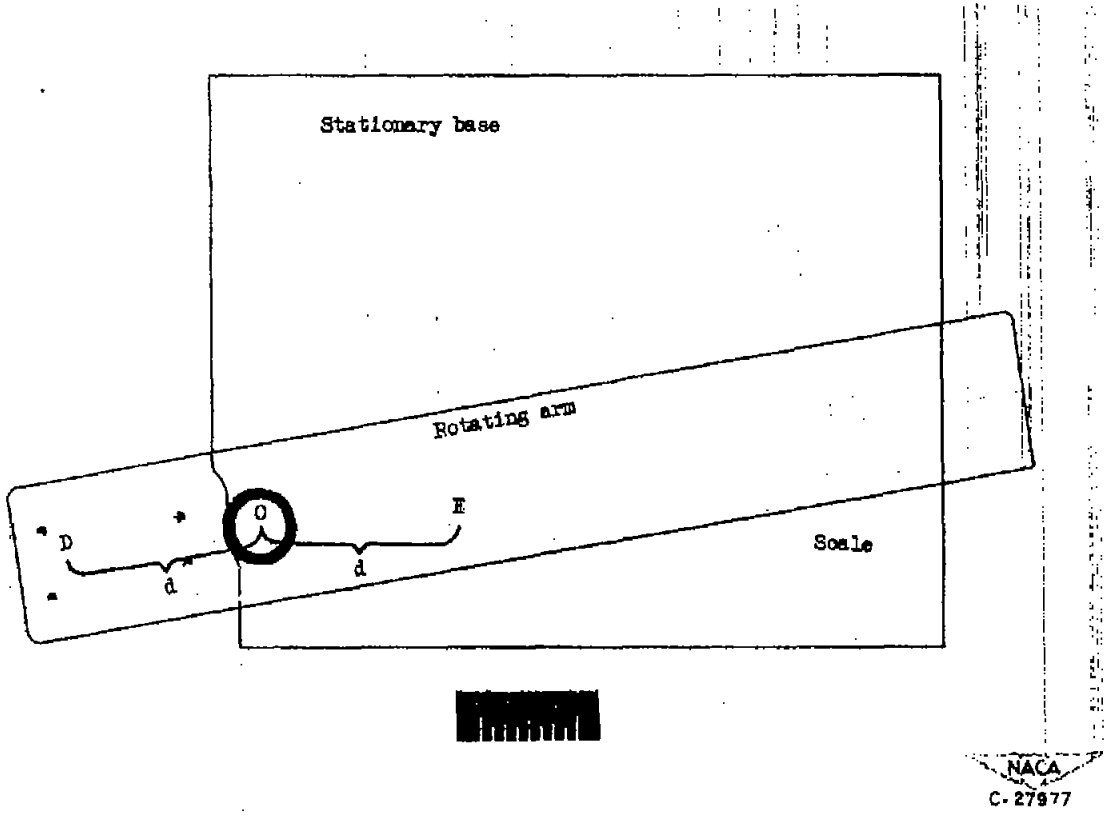

Figure 7. - Photograph of radiometer.

NACA-Langley - 10-3-51 - 325